# Linear Free Energy Relationships Associated with Hydride Transfer From [(6,6'-R<sub>2</sub>-bpy)Re(CO)<sub>3</sub>H]: A Cautionary Tale in Identifying Hydrogen Bonding Effects in the Secondary Coordination Sphere

Matthew R. Elsby, <sup>a</sup> Abhishek Kumar, <sup>a</sup> Lee M. Daniels, <sup>b</sup> Mehmed Z. Ertem, <sup>c,\*</sup> Nilay Hazari, <sup>a,\*</sup> Brandon Q. Mercado, <sup>a</sup> & Alexandra H. Paulus<sup>a</sup>

<sup>a</sup>Department of Chemistry, Yale University, New Haven, Connecticut 06520, United States of America. Email: nilay.hazari@yale.edu

<sup>b</sup>Rigaku Oxford Diffraction, The Woodlands, Texas 77381, United States of America.

<sup>c</sup>Chemistry Division, Brookhaven National Laboratory, Upton, New York 11973, United States of America. Email: mzertem@bnl.gov

#### **Abstract**

Six rhenium hydride complexes,  $[(6,6'-R_2-bpy)Re(CO)_3H]$  (bpy = 2,2'-bipyridine, R = OEt, OMe, NHMe, Me, F, Br), were synthesized. These complexes insert CO<sub>2</sub> to form rhenium formate complexes of the type [(6,6'-R<sub>2</sub>-bpy)Re(CO)<sub>3</sub>{OC(O)H}]. All the rhenium formate species were characterized using X-ray crystallography, which revealed that the bpy ligand is not co-planar with the metal coordination plane containing the two nitrogen donors of the bpy ligand but tilted. A solid-state structure of [(6,6'-Me<sub>2</sub>-bpy)Re(CO)<sub>3</sub>H] determined using MicroED also featured a tilted bpy ligand. The kinetics of CO<sub>2</sub> insertion into complexes of the type [(6,6'-R<sub>2</sub>-bpy)Re(CO)<sub>3</sub>H] were measured experimentally and the thermodynamic hydricities of [(6,6'-R<sub>2</sub>-bpy)Re(CO)<sub>3</sub>H] species were determined using theoretical calculations. A Brønsted plot constructed using the experimentally determined rate constants for CO<sub>2</sub> insertion and the calculated thermodynamic hydricities for [(6,6'-R<sub>2</sub>-bpy)Re(CO)<sub>3</sub>H] revealed a linear free energy relationship (LFER) between thermodynamic and kinetic hydricity. This LFER is different to the previously determined relationship for CO<sub>2</sub> insertion into complexes of the type [(4,4'-R<sub>2</sub>-bpy)Re(CO)<sub>3</sub>H]. At a given thermodynamic hydricity, CO<sub>2</sub> insertion is faster for complexes containing a 6,6'-substituted bpy ligand. This is likely in part due to the tilting observed for systems with 6,6'-substituted bpy ligands. Notably, the 6,6'-(NHMe)<sub>2</sub>-bpy ligand could in principle stabilize the transition state for CO<sub>2</sub> insertion via hydrogen bonding. This work shows that if only the rate of CO<sub>2</sub> insertion into [(6,6'-(NHMe)<sub>2</sub>-bpy)Re(CO)<sub>3</sub>H] is compared to [(4,4'-R<sub>2</sub>-bpy)Re(CO)<sub>3</sub>H] systems, the increase in rate could be easily attributed to hydrogen bonding, but in fact all 6,6'-substituted systems lead to faster than expected rates.

#### Introduction

Transition metal hydrides are critical intermediates in a wide array of catalytic processes that have many industrial applications.<sup>1</sup> For example, they are proposed intermediates in transition metal catalyzed hydrogenation,<sup>2</sup> hydroformylation,<sup>3</sup> alkene isomerization,<sup>4</sup> and hydrosilylation reactions,<sup>5</sup> which are relevant to diverse areas such as energy storage, the synthesis of pharmaceuticals, and the preparation of monomers for polymerization. The transfer of a hydride from a transition metal hydride to a substrate is the turnover limiting step in many of these reactions, and consequently increased understanding of this elementary step could facilitate the development of improved catalysts.

Linear free energy relationships (LFERs), which correlate the thermodynamic driving force of a reaction with the kinetic rate of a reaction, are a powerful tool in catalyst development. As part of our efforts to understand hydride transfer reactions and design improved catalysts for the conversion of CO<sub>2</sub> into commodity chemicals and fuels, we recently measured the kinetics of CO<sub>2</sub> insertion into a family of [(4,4'-R<sub>2</sub>-bpy)Re(CO)<sub>3</sub>H] (bpy = 2,2'-bipyridine; R = OMe, <sup>t</sup>Bu, Me, H, Br, COOMe, CF<sub>3</sub>) complexes to form [(4,4'-R<sub>2</sub>-bpy)Re(CO)<sub>3</sub>{OC(O)H}] (Figure 1a). We selected bpy ligated Re systems because complexes of the type [(bpy)Re(CO)<sub>3</sub>Cl] are some of the most prominent examples of homogeneous photo- or electrochemical catalysts for CO<sub>2</sub> reduction. 8 They give high selectivity to CO, are relatively stable, and species with both electron withdrawing and donating bpy ligands can readily be synthesized and characterized. The CO<sub>2</sub> insertion reactions we studied provide insight into the rate of hydride transfer because the rate-determining step is nucleophilic attack of the hydride on CO<sub>2</sub>. Using computational methods, we determined the thermodynamic hydricities of the Re hydrides. Subsequently, by correlating thermodynamic and kinetic hydricity, it was established that LFERs exist between thermodynamic and kinetic hydricity for CO<sub>2</sub> insertion into [(4,4'-R<sub>2</sub>-bpy)Re(CO)<sub>3</sub>H] in a range of solvents.<sup>9</sup> Specifically, as the thermodynamic hydricity of the Re hydride increases hydride transfer becomes faster.

The active sites of metalloenzymes often contain precisely positioned hydrogen bonding groups in their secondary coordination sphere that can interact with substrates and cause increases in activity and selectivity through stabilization of the transition state (TS).<sup>10</sup> This has inspired the design of numerous transition metal catalysts that feature hydrogen bonding functional groups in the secondary coordination sphere, which often has resulted in improved catalytic activity.<sup>11</sup> For

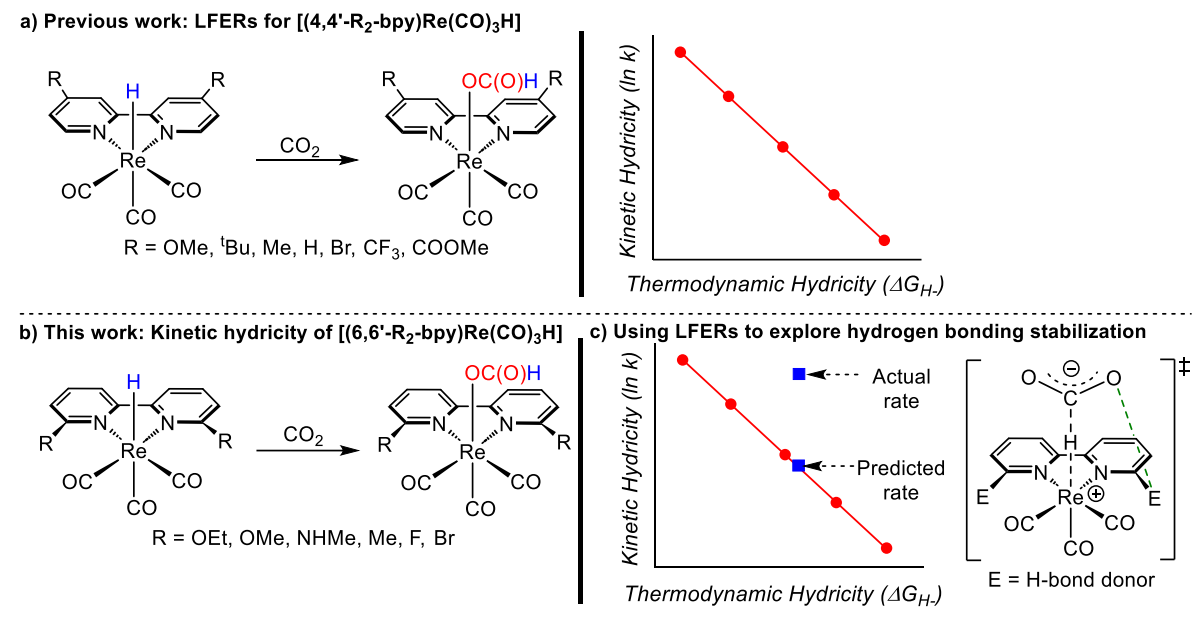


**Figure 1: a)** Previous work on CO<sub>2</sub> insertion into  $[(4,4'-R_2-bpy)Re(CO)_3H]$  to CO<sub>2</sub> showing a linear free energy relationship (LFER) between kinetic and thermodynamic hydricity. Kinetic hydricity is the rate constant for hydride transfer from a hydride donor to a hydride acceptor, while thermodynamic hydricity,  $\Delta G^{o}_{H-}$ , is the free energy required to release a free hydride ion from a metal hydride in solution. This work: **b)** Measuring rate constants for CO<sub>2</sub> insertion into  $[(6,6'-R_2-bpy)Re(CO)_3H]$  complexes, and **c)** Investigating whether a hydrogen bonding group in the secondary coordination sphere of the complex can break the LFER between kinetic and thermodynamic hydricity. The red points represent complexes without a hydrogen bond donor, whereas the blue point represents a complex with a hydrogen bond donor. The structure shows the proposed stabilization of the negatively charged carboxylate in the rate limiting TS for CO<sub>2</sub> insertion via hydrogen bonding interactions, which should lead to an increase in rate compared to the predicted value from the LFER.

example, in transition metal catalyzed CO<sub>2</sub> hydrogenation, it has been proposed that hydrogen bond donors in the ancillary ligand can increase the rate of CO<sub>2</sub> insertion into metal hydrides, leading to faster catalysis. <sup>12</sup> However, modifications to the secondary coordination sphere can also affect the primary coordination sphere by changing the electronic or steric properties of the donor atoms. Therefore, it is difficult to evaluate whether primary or secondary coordination sphere effects (or a combination of both) are causing an improvement in catalysis, especially when information about the rate of the turnover limiting elementary step is unavailable.

In principle, the LFERs we developed for  $CO_2$  insertion into  $[(4,4'-R_2-bpy)Re(CO)_3H]$  complexes provide an opportunity to assess and quantify the impact of secondary coordination sphere effects on  $CO_2$  insertion. This is because the LFER predicts the kinetic hydricity based on the thermodynamic hydricity for any complex. However, a secondary coordination sphere effect, such as hydrogen bonding should predominantly affect the TS (lowering  $\Delta G^{\ddagger}$ ) rather than the thermodynamic hydricity. Thus, a system with secondary coordination sphere stabilization of the TS should result in a deviation from the LFER for systems without secondary coordination effects

(Figure 1c). Importantly, the deviation from the expected kinetic value caused by the secondary coordination sphere effect will account for any change in thermodynamic hydricity, allowing for the disambiguation of kinetic and thermodynamic effects.

In this work, we measure the rates of CO<sub>2</sub> insertion into a series of Re hydrides featuring 6,6'substituted bpy ligands, [(6,6'-R<sub>2</sub>-bpy)Re(CO)<sub>3</sub>H] (R = OEt, OMe, NHMe, Me, F, Br) and use theoretical calculations to determine their thermodynamic hydricities (Figure 1b). This enables the elucidation of a LFER between kinetic and thermodynamic hydricity for CO<sub>2</sub> insertion into complexes of the type [(6,6'-R<sub>2</sub>-bpy)Re(CO)<sub>3</sub>H]. Notably, the LFER for insertion into complexes with 6,6'-substituted bpy ligands is different than the LFER we previously determined for 4,4'substituted bpy ligands, with faster CO<sub>2</sub> insertion observed for 6,6'-substituted bpy ligands at the same thermodynamic driving force. The general increase in rate is especially significant for interpreting the effect of the 6,6'-(NHMe)<sub>2</sub>-bpy ligand. This ligand was used to test the hypothesis that the N-H group could stabilize the key TS for CO<sub>2</sub> insertion by stabilizing the negative charge on the carboxylate through hydrogen bonding (Figure 1c), as has been proposed in other CO<sub>2</sub> insertion reactions. 12c,13 Our work shows that if the rate of CO<sub>2</sub> insertion into [(6,6'-(NHMe)<sub>2</sub>bpy)Re(CO)<sub>3</sub>H] was only compared with the rates of CO<sub>2</sub> insertion into [(4,4'-R<sub>2</sub>-bpy)Re(CO)<sub>3</sub>H] complexes it would be easy to incorrectly conclude that hydrogen bonding was in fact leading to an increase in rate. Instead, when the complete set of 6,6'-substituted bpy ligands are considered, the 6,6'-(NHMe)<sub>2</sub>-bpy ligand is not a significant outlier. Thus, this work both provides a method to increase the rate of CO<sub>2</sub> insertion into bpy-ligated Re hydrides at a particular thermodynamic driving force and highlights the need to perform rigorous control experiments to identify hydrogenbond stabilization of a TS.

#### **Results and Discussion**

Synthesis of Re complexes with 6,6'-substituted bpy ligands

Based on analysis of crystal structures of [(6,6'-R<sub>2</sub>-bpy)Re(CO)<sub>3</sub>Cl] complexes,<sup>14</sup> we proposed that the presence of functional groups containing N–H bonds in the 6 or 6' positions of bpy could result in hydrogen bonding interactions that stabilize the negative charge on the carboxylate in the TS for CO<sub>2</sub> insertion into a Re hydride in a complex of the form [(6,6'-R<sub>2</sub>-bpy)Re(CO)<sub>3</sub>H] (Figure 1c). To test our hypothesis, we targeted the complex [(6,6'-(NHMe)<sub>2</sub>-bpy)Re(CO)<sub>3</sub>H]. Initially, we followed a literature procedure to synthesize [(6,6'-(NHMe)<sub>2</sub>-bpy)Re(CO)<sub>3</sub>Cl] through a reaction

of [6,6'-(NHMe)<sub>2</sub>-bpy] with [Re(CO)<sub>5</sub>Cl] in refluxing toluene (Scheme 1).<sup>14a</sup> Subsequent treatment of [(6,6'-(NHMe)<sub>2</sub>-bpy)Re(CO)<sub>3</sub>Cl] with AgOTf generated [(6,6'-(NHMe)<sub>2</sub>-bpy)Re(CO)<sub>3</sub>(OTf)] (Scheme 1), which was converted into [(6,6'-(NHMe)<sub>2</sub>-bpy)Re(CO)<sub>3</sub>H] via a reaction with NaBH<sub>4</sub>. To generally understand the impact of 6,6'-bpy substituents on CO<sub>2</sub> insertion into [(6,6'-R<sub>2</sub>-

**Scheme 1:** Synthesis of [(6,6'-R<sub>2</sub>-bpy)Re(CO)<sub>3</sub>H] complexes.

bpy)Re(CO)<sub>3</sub>H], we used the same synthetic route to prepare complexes containing 6,6'-ethoxy, methoxy, methyl, fluorine, and bromine substituents on the bpy. The ethoxy and methoxy substituents were selected because they are electron donating groups that have similar electronic and steric properties to NHMe but cannot act as hydrogen bond donors. Unfortunately, attempts to prepare a Re hydride with a 6,6'-(NMe<sub>2</sub>)<sub>2</sub>-bpy ligand were unsuccessful. Methyl, fluorine, and bromine substituents were included to provide some variation in the electron-donating ability of the 6,6'-substituent, while keeping steric factors relatively constant.

All our new Re hydrides cleanly insert  $CO_2$  in acetonitrile (MeCN) to form the Re formate complexes  $[(6,6'-R_2-bpy)Re(CO)_3\{OC(O)H\}]$  (R = OEt, OMe, NHMe, Me, F, Br) (Scheme 2). For each reaction, the disappearance of the characteristic Re–H resonance in the  $^1H$  NMR spectrum ( $\delta = 0.8-1.3$  ppm) was concomitant with the appearance of a signal corresponding to a formate resonance ( $\delta \sim 8.1$  ppm). The new Re formate complexes were isolated and fully characterized, including some by single crystal X-ray diffraction. The solid-state structures of  $[(6,6'-R_2-bpy)Re(CO)_3\{OC(O)H\}]$  (R = OEt, OMe, NHMe, Br) are shown in Figure 2, while the structures

Scheme 2: Synthesis of  $[(6,6'-R_2-bpy)Re(CO)_3\{OC(O)H\}]$ .

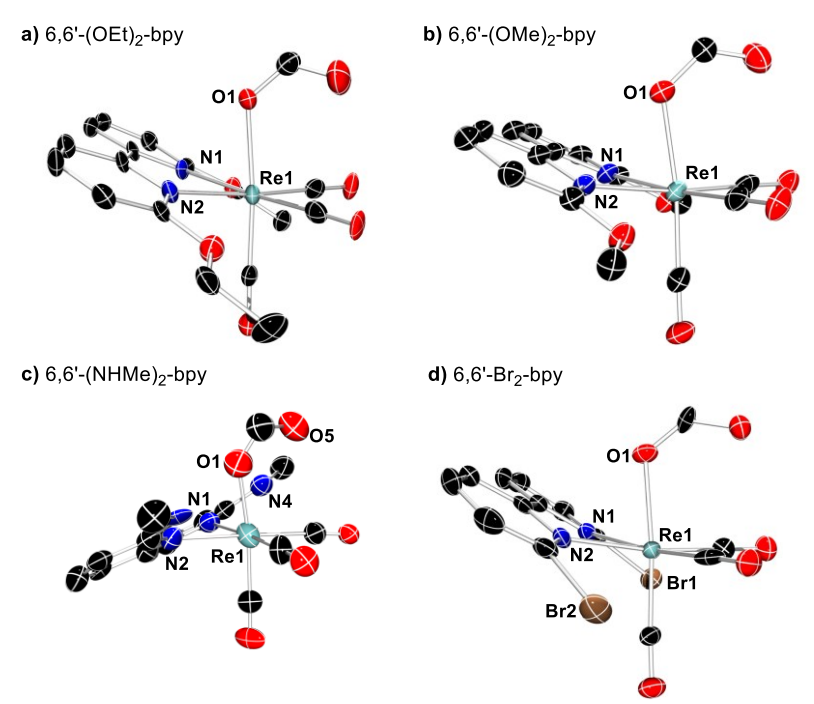


**Figure 2.** Solid state molecular structures of **a)** [(6,6'-(OEt)<sub>2</sub>-bpy)Re(CO)<sub>3</sub>{OC(O)H}]. Selected bond lengths (Å): Re(1)–N(1) 2.205(10), Re(1)–N(2) 2.201(10), Re(1)–O(1) 2.160(5). Selected bond angles (°): N(1)-Re(1)-N(2) 74.5(4); **b)** [(6,6'-(OMe)<sub>2</sub>-bpy)Re(CO)<sub>3</sub>{OC(O)H}]. Selected bond lengths (Å): Re(1)–N(1) 2.190(2), Re(1)–N(2) 2.193(3), Re(1)–O(1) 2.144(2). Selected bond angles (°): N(1)-Re(1)-N(2) 74.68(9); **c)** [(6,6'-(NHMe)<sub>2</sub>-bpy)Re(CO)<sub>3</sub>{OC(O)H}]. Selected bond lengths (Å): Re(1)–N(1) 2.212(9), Re(1)–N(2) 2.211(10), Re(1)–O(1) 2.108(9). Selected bond angles (°): N(1)-Re(1)-N(2) 73.4(3); **d)** [(6,6'-Br<sub>2</sub>-bpy)Re(CO)<sub>3</sub>{OC(O)H}]. Note that there are two crystallographically independent, chemically identical models in the asymmetric unit. The two sites are distinguished with the suffixes "A" and "B." Selected bond lengths (Å): Re(1A)–N(1A) 2.230(6), Re(1A)–N(2A) 2.215(7), Re(1A)–O(1A) 2.151(5), Re(1B)–N(1B) 2.229(6), Re(1B)–N(2B) 2.196(6), Re(1B)–O(1B) 2.147(6). Selected bond angles (°): N(1A)-Re(1A)-N(2A) 74.6(2), N(1B)-Re(1B)-N(2B) 73.7(2).

of [(6,6'-R<sub>2</sub>-bpy)Re(CO)<sub>3</sub>{OC(O)H}] (R = Me, F) are lower quality and only provide information about connectivity and qualitative trends relating to the orientation of the ligands (see section SXIV). In all cases, the Re center has the expected distorted octahedral geometry with the formate ligand *trans* to a CO ligand. Notably, the Re center and the nitrogen atoms of the 6,6'-R<sub>2</sub>-bpy ligands are not co-planar with the carbon atoms of the bpy ligand. Instead, the 6,6'-R<sub>2</sub>-bpy ligand is tilted out of the coordination plane containing the Re center, the two nitrogen donors of the 6,6'-R<sub>2</sub>-bpy ligand and the CO ligands (Figure 3). This tilting of the bpy ligand is presumably due to steric factors, as it is not observed to the same extent for related complexes containing either 4,4'-substituents or unsubstituted bpy ligands. <sup>8e,14b,15</sup> There is no clear correlation between the magnitude of the tilt, which range from 4-29°, and the %V<sub>Bur</sub> of the 6,6'-R<sub>2</sub>-bpy coordinated to a naked Re atom (see section SIX). Analysis of the solid-state structures of related Re and Mn

complexes in the literature with 6,6'-R<sub>2</sub>-bpy ligands reveals the same magnitude of tilting, although it has rarely been noted. <sup>14,16</sup>

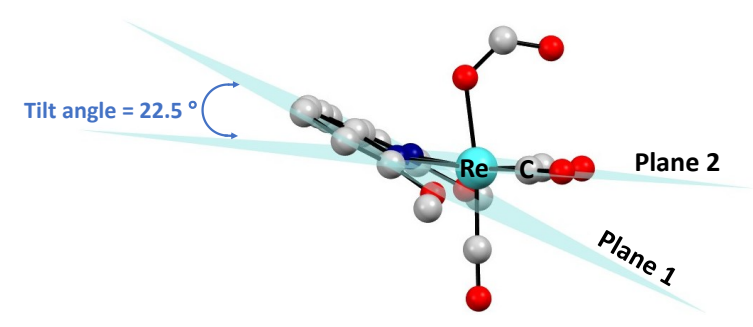


**Figure 3.** Solid state molecular structure of [(6,6'-(OMe)<sub>2</sub>-bpy)Re(CO)<sub>3</sub>{OC(O)H}] displaying the tilt angle of the bpy ligand. Plane one is comprised of the aromatic carbon and nitrogen atoms of the bpy ligand. Plane two is comprised of rhenium, the equatorial carbon atoms of the carbonyl ligands, and the nitrogen atoms of bpy. The tile angle is plane one – plane two.

**Table 1:** Orientation and tilt angle of bpy in  $[(6,6'-R_2-bpy)Re(CO)_3\{OC(O)H\}]$  complexes. Note: tilted down is denoted as the R-substituents oriented towards the axial carbonyl ligand. There are two values for Br since Z'=2.

6,6'-R <sub>2</sub> -bpy	bpy tilt angle (°)	bpy orientation
R = OEt	18.4	Down
R = OMe	22.5	Down
R = NHMe	-29.0	Up
R = Br	26.9	Down
	30.4	Down

In principle, the  $6.6'-R_2$ -bpy ligand in complexes of the type  $[(6.6'-R_2-bpy)Re(CO)_3\{OC(O)H\}]$  can tilt either so the 6.6'-substituents are on the same side of the coordination plane as the formate ligand (defined here as up, negative tilt) or on the same side of the coordination plane as the CO ligand that is *trans* to the formate ligand (defined here as down, positive tilt). Analysis of the solid-state structures of  $[(6.6'-R_2-bpy)Re(CO)_3\{OC(O)H\}]$  reveals that the  $6.6'-R_2$ -bpy tilts down for all substituents except NHMe, where it points up (Tables 1 and S1). This raises the possibility of hydrogen bonding between the N–H group and formate ligand and the distance between N4 and O5 is 2.926(15) Å, which is within typical hydrogen bonding distance. Nevertheless, the close solid state distance could be influenced by packing effects. Therefore, it is notable that the chemical shift in the  $^1$ H NMR spectrum of the proton associated with the NHMe substituent in  $[(6.6'-(NHMe)_2-bpy)Re(CO)_3\{OC(O)H\}]$  is shifted downfield by approximately 1 ppm compared the chemical shift of  $[(6.6'-(NHMe)_2-bpy)Re(CO)_3X]$  (X = H or Cl), which is consistent with hydrogen bonding. However, a NOESY experiment did not reveal any correlation between the N–H substituent and the C–H of bound formate and the IR stretching frequency of the N–H vibrations

in [(6,6'-(NHMe<sub>2</sub>-bpy)Re(CO)<sub>3</sub>{OC(O)H}] and [(6,6'-(NHMe)<sub>2</sub>-bpy)Re(CO)<sub>3</sub>H] are similar, suggesting no hydrogen bonding.<sup>19</sup> Further, no changes were observed at low temperature in the <sup>1</sup>H NMR spectrum, where it may be expected that hydrogen bonding between one NHMe substituent and the formate ligand, would make the two sides of the 6,6'-(NHMe)<sub>2</sub>-bpy ligand inequivalent. Overall, the experimental data is inconclusive about whether there is a hydrogen bond between the NH group of 6,6'-(NHMe)<sub>2</sub>-bpy and the formate ligand.

To evaluate whether the observed tilting of the 6,6'-R<sub>2</sub>-bpy ligand is due to the presence of the formate ligand, we attempted to structurally characterize our Re hydrides. Unfortunately, complexes of the type [(6,6'-R<sub>2</sub>-bpy)Re(CO)<sub>3</sub>H] are light sensitive in solution, and the majority of attempts to obtain crystals of sufficient quality for X-ray diffraction resulted in microcrystalline powders. The only complex we were able to obtain high-quality X-ray data for was [(6,6'-Br<sub>2</sub>-bpy)Re(CO)<sub>3</sub>H] (Figure 4a). The structure of [(6,6'-Br<sub>2</sub>-bpy)Re(CO)<sub>3</sub>H] shows the same tilt down 25.9°) observed in almost all the Re formate complexes, indicating that the origin of the tilt is likely due to steric factors associated with the 6,6'-R<sub>2</sub>-bpy ligand. The hydride in [(6,6'-Br<sub>2</sub>-bpy)Re(CO)<sub>3</sub>H] was located in the Fourier map and the Re–H bond length is 1.85(9) Å. This is consistent with the bond length computed using theoretical calculations (1.790 Å) (*vide infra*).

To attempt to determine the solid-state structure of other [(6,6'-R<sub>2</sub>-bpy)Re(CO)<sub>3</sub>H] complexes, we turned to microcrystal electron diffraction (MicroED).<sup>20</sup> MicroED is a hybrid method, which exploits the advantages of both electron microscopy and crystallography, and uses an electron beam to generate a diffraction map. It is ideally suited to microcrystalline samples and does not have the same inherent problems locating metal hydrides as X-ray diffraction.<sup>21</sup> We obtained MicroED data for [(6,6'-Me<sub>2</sub>-bpy)Re(CO)<sub>3</sub>H] (Figure 4b),<sup>22</sup> which is a rare example of a metal

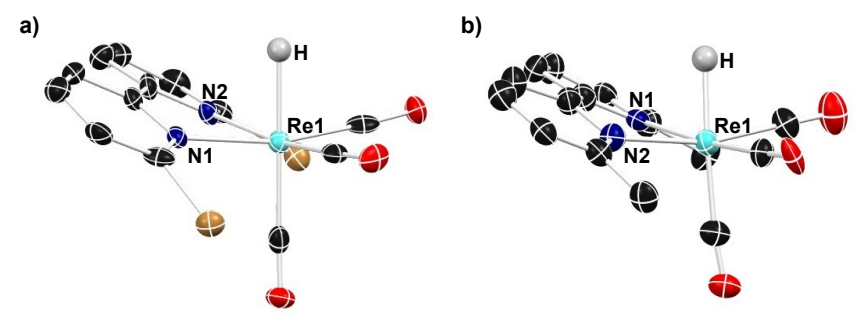


**Figure 4.** Solid state molecular structures of **a)**  $[(6,6'-Br_2-bpy)Re(CO)_3H]$  from single X-ray crystallography. Selected bond lengths (Å): Re(1)-N(1) 2.207(10), Re(1)-N(2) 2.206(10), Re(1)-H 1.85(9). Selected bond angles (°): N(1)-Re(1)-N(2) 74.4(4); **b)**  $[(6,6'-R_2-bpy)Re(CO)_3H]$  from MicroED. Selected bond lengths (Å): Re(1)-N(1) 2.25(3), Re(1)-N(2) 2.26(3), Re(1)-H 1.79(8). Selected bond angles (°): N(1)-Re(1)-N(2) 74.8(12).

hydride that has been structurally characterized using MicroED.<sup>21</sup> The same downward tilting of the 6,6'-Me<sub>2</sub>-bpy ligand (25.5°) is observed as in the formate complex, which is consistent with our hypothesis that the steric bulk of 6,6'-R<sub>2</sub>-bpy ligand causes the tilting. The Re–H bond length in [(6,6'-Me<sub>2</sub>-bpy)Re(CO)<sub>3</sub>H] is 1.80(7) Å, which is consistent with the computed bond length of 1.794 Å.

To further understand the tilting of the 6,6'-R<sub>2</sub>-bpy ligand in  $[(6,6'-R_2-bpy)Re(CO)_3X]$  (X = OC(O)H or H) type complexes and evaluate if hydrogen bonding is present in [(6,6'-(NHMe)<sub>2</sub>bpy)Re(CO)<sub>3</sub>{OC(O)H}] we performed density functional theory calculations at the M06 level of theory<sup>23</sup> (see section SXIII). In all our optimized structures the 6,6'-R<sub>2</sub>-bpy ligand is tilted, indicating that this distortion is intrinsic to the complexes and not a crystal packing effect. For all complexes containing a formate ligand, including the 6,6'-(NHMe)<sub>2</sub>-bpy ligand, theory predicts it is energetically favorable for the 6,6'-R<sub>2</sub>-bpy ligand to tilt down (Table 2). The energy difference between the up and down isomers ranges from -0.3 to -4.1 kcal mol<sup>-1</sup>, with the smallest difference occurring for [(6,6'-(NHMe)<sub>2</sub>-bpy)Re(CO)<sub>3</sub>{OC(O)H}]. This suggests that the observation of the up isomer of [(6,6'-(NHMe)<sub>2</sub>-bpy)Re(CO)<sub>3</sub>{OC(O)H}] in the solid-state structure is a function of crystallization, as opposed to a large energy preference for the up isomer, indicating that hydrogen bonding is not important. Consistent with this theory, theoretical calculations indicate that the up isomer of [(6,6'-(NHMe)<sub>2</sub>-bpy)Re(CO)<sub>3</sub>H], where there cannot be any hydrogen bonding, is preferred by 0.4 kcal mol<sup>-1</sup>. For all other Re hydrides the down isomer is preferred. The exact reasons why the up or down isomer is preferred for any given complex are unclear. An expected consequence of the tilting is that the 6,6'-substituted bpy ligand is a worse  $\sigma$ -donor because the lone pairs on nitrogen donor of the bpy are not as well-aligned with the metal d-orbitals, as when the bpy ligand is fully planar. This is further supported by Natural Population Analysis (NPA) data

**Table 2:** Theoretical calculations at the M06 level of theory comparing the energetic difference between the up and down isomers of  $6.6'-R_2$ -bpy ligated Re hydride and formate complexes.

	ΔG between up and down isomers (G <sub>down</sub> - G <sub>up</sub> ) (kcal mol <sup>-1</sup> )			
6,6'-R <sub>2</sub> -bpy	Re-H	Re-{OC(H)O}		
R = OEt	ND*	ND*		
R = OMe	ND*	-4.1		
R = NHMe	0.4	-0.3		
R = Me	-2.5	-2.7		
R = Br	-4.4	-1.0		

<sup>\*</sup>ND = not determined because only a single configuration (down isomer) was found, so it was not possible to calculate an energy difference between isomers.

showing that the Re- $N_{bpy}$  bond orders decrease for 6,6'- $R_2$ -bpy ligated Re hydride and solvento complexes with tilting compared to planar 4,4'- $R_1$ -bpy complexes for the same substituents (R = Br, Me, OMe). In contrast, the computed bond orders of the remaining coordination sites around the Re center are essentially the same (Tables S5 & S6). Overall, our data shows that adding 6,6'-substituents to the bpy ligand significantly changes the structural parameters around Re.

## Kinetics of $CO_2$ insertion into $[(6,6'-R_2-bpy)Re(CO)_3H]$

The clean insertion of CO<sub>2</sub> into complexes of the type  $[(6,6'-R_2-bpy)Re(CO)_3H]$  allowed us to perform kinetic studies to determine the rates of insertion. The kinetics of CO<sub>2</sub> insertion into  $[(6,6'-R_2-bpy)Re(CO)_3H]$  were measured using a stopped-flow instrument with a UV-Vis detector in MeCN at 30 °C. An excess of CO<sub>2</sub> (>20 equiv.) was used to ensure pseudo-first order conditions. Representative kinetic profiles and analysis are shown in Figures S1 and S2. The reactions are first-order in [Re] and [CO<sub>2</sub>], to give an overall rate law of  $k_1[(6,6'-R_2-bpy)Re(CO)_3H][CO_2]$  (see Figure S3), which is consistent with other examples of CO<sub>2</sub> insertion into metal hydrides.<sup>7,24</sup> For each reaction, the value of  $k_1$  was obtained (see Table 3 by dividing the  $k_{obs}$  value (determined from a plot of  $ln[(6,6'-R_2-bpy)Re(CO)_3H]$  vs. time) by the concentration of CO<sub>2</sub>.

**Table 3:** Rate constants and activation parameters for CO<sub>2</sub> insertion into [(6,6'-R<sub>2</sub>-bpy)Re(CO)<sub>3</sub>H] in MeCN at 303 K.

Complex	$k_1 (M^{-1}s^{-1})^a$	ΔH <sup>‡</sup> (kcal mol <sup>-1</sup> )	ΔS <sup>‡</sup> (cal mol <sup>-1</sup> K <sup>-1</sup> )	ΔG <sup>‡</sup> 303 (kcal mol <sup>-1</sup> )
[(6,6'-(OEt) <sub>2</sub> -bpy)Re(CO) <sub>3</sub> H]	8.0 x 10 <sup>-1</sup>	$9.5 \pm 1.0$	$-27.8 \pm 2.3$	$17.9 \pm 1.7$
$[(6,6'\text{-}(OMe)_2\text{-}bpy)Re(CO)_3H]$	6.1 x 10 <sup>-1</sup>	$10.3\pm1.0$	$-24.1 \pm 2.4$	$17.6 \pm 1.7$
[(6,6'-(NHMe) <sub>2</sub> -bpy)Re(CO) <sub>3</sub> H]	$3.7 \times 10^{-1}$	$9.6\pm1.0$	$\textbf{-29.0} \pm 2.9$	$18.4\pm1.8$
$[(6,6'\text{-Me}_2\text{-bpy})\text{Re}(\text{CO})_3\text{H}]$	2.0 x 10 <sup>-2</sup>	$10.4\pm1.0$	$\textbf{-32.0} \pm 3.2$	$20.1\pm2.0$
$[(6,6'-F_2-bpy)Re(CO)_3H]$	1.7 x 10 <sup>-2</sup>	$9.0 \pm 0.9$	$\textbf{-37.0} \pm 3.7$	$20.2\pm2.0$
$[(6,6'-Br_2-bpy)Re(CO)_3H]$	$8.4 \times 10^{-3}$	$9.6 \pm 1.0$	$-36.5 \pm 3.7$	$20.6 \pm 2.1$

<sup>&</sup>lt;sup>a</sup>The errors associated with the  $k_1$  values are  $\pm 5\%$ .

The rates of CO<sub>2</sub> insertion qualitatively trend with the electron richness of the 6,6'-bpy substituents. The fastest rates are obtained with complexes containing OEt and OMe substituted bpy ligands, while the slowest rate is obtained with the Br substituted bpy ligand. This is consistent with results for complexes of the type [(4,4'-R<sub>2</sub>-bpy)Re(CO)<sub>3</sub>H] where there was a strong correlation between CO<sub>2</sub> insertion rates and the electron richness of the 4,4'-bpy ligand as evidenced by a Hammett plot.<sup>7</sup> Unfortunately, due to steric effects *ortho* Hammett parameters do not exist and our efforts to estimate approximate Hammett parameters for the 6,6'-bpy ligands using first reduction potentials as demonstrated by Kubiak *et al.*<sup>25</sup> were unsuccessful (see section SX). Based only on the

measured rate constants it is not clear if hydrogen bonding is increasing the rate of CO<sub>2</sub> insertion into  $[(6,6'-(NHMe)_2-bpy)Re(CO)_3H]$  ( $k_I = 3.7 \times 10^{-1} \text{ M}^{-1}\text{s}^{-1}$ ) as it fits within the range observed for other complexes with 6,6'-bpy ligands, although it is faster than any Re hydride we studied with a 4,4'-bpy ligand.<sup>7</sup> The slightly faster rate for  $[(6,6'-(OEt)_2-bpy)Re(CO)_3H]$  ( $k_I = 8.0 \times 10^{-1} \text{ M}^{-1}\text{s}^{-1}$ ) compared to  $[(6,6'-(OMe)_2-bpy)Re(CO)_3H]$  ( $k_I = 6.1 \times 10^{-1} \text{ M}^{-1}\text{s}^{-1}$ ) suggests that steric factors may be relevant for CO<sub>2</sub> insertion into our complexes containing 6,6'-bpy substituents. No trends were observed when comparing Re hydrides containing 6,6'-substituted bpy ligands with those containing 4,4'-substituted bpy ligands with the same substituent. For example, the rate constant for CO<sub>2</sub> insertion into  $[(6,6'-(OMe)_2-bpy)Re(CO)_3H]$  ( $k_I = 6.1 \times 10^{-1} \text{ M}^{-1}\text{s}^{-1}$ ) was faster than the rate constant for insertion into  $[(4,4'-(OMe)_2-bpy)Re(CO)_3H]$  ( $k_I = 2.2 \times 10^{-1} \text{ M}^{-1}\text{s}^{-1}$ ) was slower than the rate constant for insertion into  $[(4,4'-(OMe)_2-bpy)Re(CO)_3H]$  ( $k_I = 2.0 \times 10^{-2} \text{ M}^{-1}\text{s}^{-1}$ ) was slower than the rate constant for insertion into  $[(4,4'-(OMe)_2-bpy)Re(CO)_3H]$  ( $k_I = 1.1 \times 10^{-1} \text{ M}^{-1}\text{s}^{-1}$ ).

To gain further insight about CO<sub>2</sub> insertion into complexes of the type [(6,6'-R<sub>2</sub>-bpy)Re(CO)<sub>3</sub>H] we used Eyring analysis to determine the activation parameters (Table 3). For all systems negative entropies of activation ( $\Delta S^{\ddagger}$ ) were observed, ranging from -24.1  $\pm$  2.4 for [(6,6'-(OMe)<sub>2</sub>bpy)Re(CO)<sub>3</sub>H] to  $-37.0 \pm 3.7$  cal mol<sup>-1</sup> K<sup>-1</sup> for [(6,6'-F<sub>2</sub>-bpy)Re(CO)<sub>3</sub>H], a surprisingly large difference of greater than 10 cal mol<sup>-1</sup> K<sup>-1</sup>. The negative entropy of activation is consistent with a process in which two molecules are converted into one and the values are comparable to those reported for other examples of CO<sub>2</sub> insertion into metal hydrides.<sup>26</sup> It is unclear why the difference between entropies of activation for our family of 6,6'-substituted bpy complexes is greater than 10 cal mol<sup>-1</sup> K<sup>-1</sup> and there appear to be no trends in the entropy of activation based on the electronic or steric properties of the 6,6'-substituent. Interestingly, an even larger range of activation entropies, ~15 cal mol<sup>-1</sup> K<sup>-1</sup>, was observed for CO<sub>2</sub> insertion into complexes of the type [(4,4'-R<sub>2</sub>bpv)Re(CO)<sub>3</sub>H].<sup>7</sup> However, in the case of complexes of the type [(4,4'-R<sub>2</sub>-bpy)Re(CO)<sub>3</sub>H] the entropies of activation are significantly more negative than for [(6,6'-R<sub>2</sub>-bpy)Re(CO)<sub>3</sub>H] complexes, as in most cases the values are lower than -40 cal mol<sup>-1</sup> K<sup>-1</sup>. This indicates that the transition state for insertion into hydrides containing 6,6'-substituted bpy ligands is less ordered than for insertion into complexes containing 4,4'-substituted bpy ligands. The enthalpies of activation (ΔH<sup>‡</sup>) are much smaller for CO<sub>2</sub> insertion into complexes of the type [(4.4'-R<sub>2</sub>bpy)Re(CO)<sub>3</sub>H], (typically below 9 kcal mol<sup>-1</sup>)<sup>7</sup> compared to insertion into [(6,6'-R<sub>2</sub>-

bpy)Re(CO)<sub>3</sub>H], where the numbers range from  $9.0 \pm 0.9$  for [(6,6'-F<sub>2</sub>-bpy)Re(CO)<sub>3</sub>H] to  $10.4 \pm 1.0$  for [(6,6'-Me<sub>2</sub>-bpy)Re(CO)<sub>3</sub>H]. We hypothesize that the tilting of the bpy ring in systems with 6,6'-substituents may be responsible for the change in activation parameters, as it likely effects both the donor power of the bpy ligand, which could impact  $\Delta H^{\ddagger}$ , and solvent ordering around the complex, which could impact  $\Delta S^{\ddagger}$ . Consistent with this hypothesis the most negative entropy of activation is observed for [(6,6'-F<sub>2</sub>-bpy)Re(CO)<sub>3</sub>H], which has the least tilting of the bpy ligand. The similar activation parameters for [(6,6'-(NHMe)<sub>2</sub>-bpy)Re(CO)<sub>3</sub>H] in comparison to other 6,6'-substituted complexes suggest that there is no hydrogen bonding interaction in the TS for the case of the 6,6'-(NHMe)<sub>2</sub>-bpy ligand.

Kinetic isotope effects (KIE) can be valuable for understanding the mechanism of CO<sub>2</sub> insertion into metal hydrides<sup>24</sup> and in the case of our series of 6,6'-substituted complexes could provide information about whether the N-H group in [(6,6'-(NHMe)<sub>2</sub>-bpy)Re(CO)<sub>3</sub>H] plays an active role in stabilizing the transition state for insertion. Initially, we compared the KIEs  $(k_{\rm H}/k_{\rm D})$  for CO<sub>2</sub> insertion into [(6,6'-(OEt)<sub>2</sub>-bpy)Re(CO)<sub>3</sub>H] and [(6,6'-(NHMe)<sub>2</sub>-bpy)Re(CO)<sub>3</sub>H], by synthesizing [(6,6'-(OEt)<sub>2</sub>-bpy)Re(CO)<sub>3</sub>D] and [(6,6'-(NDMe)<sub>2</sub>-bpy)Re(CO)<sub>3</sub>D], respectively (Figure 5). KIEs of  $0.62 \pm 0.06$  and  $0.54 \pm 0.05$  were observed for [(6,6'-OEt<sub>2</sub>-bpy)Re(CO)<sub>3</sub>H] and [(6,6'-(NHMe)<sub>2</sub>bpy)Re(CO)<sub>3</sub>H], respectively. This suggests that the mechanism for CO<sub>2</sub> insertion is similar between the two complexes and the inverse KIEs are consistent with what has been observed for CO<sub>2</sub> insertions into complexes of the type [(4,4'-R<sub>2</sub>-bpy)Re(CO)<sub>3</sub>H] and other transition metal hydride complexes. 7,24,26b,26c The primary origin of the inverse KIE is that the strength of the C-H bond formed is greater than the strength of the M-H bond broken. To probe the potential impact of hydrogen bonding in [(6,6'-(NHMe)<sub>2</sub>-bpy)Re(CO)<sub>3</sub>H], we synthesized [(6,6'-(NDMe)<sub>2</sub>bpy)Re(CO)<sub>3</sub>H], in which only the amines on the ligand were deuterated. A KIE of 1.1  $\pm$  0.1 was observed when comparing [(6,6'-(NHMe)<sub>2</sub>-bpy)Re(CO)<sub>3</sub>H] with [(6,6'-(NDMe)<sub>2</sub>-bpy)Re(CO)<sub>3</sub>H], suggesting that hydrogen bonding is not impacting the reaction.

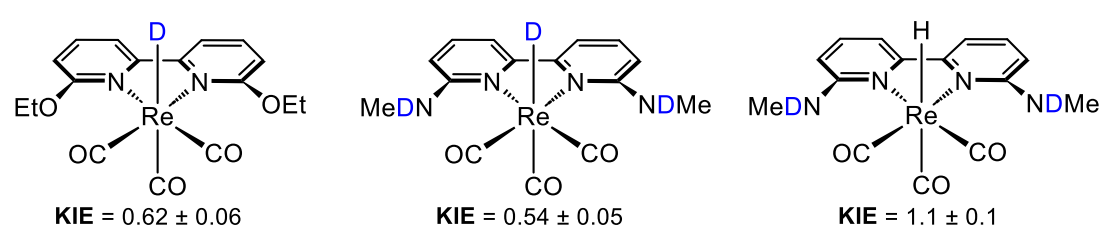


Figure 5: KIE  $(k_{\rm H}/k_{\rm D})$  associated with CO<sub>2</sub> insertion into different 6,6'-R<sub>2</sub>-bpy substituted Re hydrides.

Kinetics of hydride transfer from  $[(6,6'-R_2-bpy)Re(CO)_3H]$  to 1,3-dimethyl-pyridin-1-ium (NMP<sup>+</sup>) A potential problem with using 6,6'-substituted bpy ligands is that steric factors could lead to slower rates of reaction. Given that the rates of CO<sub>2</sub> insertion into 6,6'-substituted bpy Re hydrides were generally comparable to 4,4'-substituted bpy Re hydrides with the same substituents, this is likely not an issue for CO<sub>2</sub>. To gain more insight into the impact of steric factors on the rates of hydride transfer, we measured the rates of hydride transfer from  $[(6,6'-R_2-bpy)Re(CO)_3H]$  complexes to 1,3-dimethyl-pyridin-1-ium (NMP<sup>+</sup>) (Table 4). This reaction differs from CO<sub>2</sub> insertion because after hydride transfer the substituted dihydropyridine that is generated does not coordinate to the metal center and instead the product is a cationic Re acetonitrile complex. The kinetics of hydride transfer were recorded using UV-vis spectroscopy under pseudo first order conditions with an excess of NMP<sup>+</sup>. The rate law for hydride transfer is  $k_I[(6,6'-R_2-bpy)Re(CO)_3H][NMP<sup>+</sup>]$  (Figure S12).

**Table 4:** Rate constants for hydride transfer from [(6,6'-R<sub>2</sub>-bpy)Re(CO)<sub>3</sub>H] to NMP<sup>+</sup>.

Complex	$k_1 (\mathbf{M}^{-1} \mathbf{s}^{-1})^{\mathbf{a}}$
[(6,6'-(OEt) <sub>2</sub> -bpy)Re(CO) <sub>3</sub> H]	9.8 x 10 <sup>-3</sup>
$[(6,6'-(OMe)_2-bpy)Re(CO)_3H]$	$5.0 \times 10^{-2}$
$[(6,6'-(NHMe)_2-bpy)Re(CO)_3H]$	1.5 x 10 <sup>-4</sup>
$[(6,6'-Me_2-bpy)Re(CO)_3H]$	8.0 x 10 <sup>-4</sup>
$[(6,6'-F_2-bpy)Re(CO)_3H]$	1.3 x 10 <sup>-4</sup>
[(6,6'-Br <sub>2</sub> -bpy)Re(CO) <sub>3</sub> H]	2.5 x 10 <sup>-4</sup>

<sup>&</sup>lt;sup>a</sup>The errors associated with the  $k_I$  values are  $\pm 5\%$ .

As observed for CO<sub>2</sub> insertion, in general systems with more electron donating 6,6'-substituents on the bpy ligand react faster than systems with electron withdrawing substituents but there are several exceptions. For example, [(6,6'-(NHMe)<sub>2</sub>-bpy)Re(CO)<sub>3</sub>H] reacts surprisingly slowly, with a rate that is slower than [(6,6'-Br<sub>2</sub>-bpy)Re(CO)<sub>3</sub>H]. Although, this could be due to steric factors, the same decrease in rate is not observed for [(6,6'-(OMe)<sub>2</sub>-bpy)Re(CO)<sub>3</sub>H] or [(6,6'-(OEt)<sub>2</sub>-bpy)Re(CO)<sub>3</sub>H], which have comparable steric bulk. Finally, when comparing Re hydrides containing 6,6'-substituted bpy ligands with those containing 4,4'-substituted bpy ligands with the

same substituent,<sup>7</sup> the reactions of species with 6,6'-substituted bpy ligands are always slower, suggesting a general steric effect.

Computational determination of thermodynamic hydricity of  $[(6,6'-R_2-bpy)Re(CO)_3H]$  complexes and linear free energy relationships

Previous work determined that it is challenging to experimentally measure the thermodynamic hydricity of Re hydrides due to their limited stability in solution. Consequently, we performed theoretical calculations to determine the relative thermodynamic hydricity of our family of [(6,6'-R<sub>2</sub>-bpy)Re(CO)<sub>3</sub>H] complexes using isodesmic hydride exchange reactions following recently reported computational protocols (Table 5). The relative thermodynamic hydricities for the 6,6'-R<sub>2</sub>-bpy substituted bpy complexes generally follow the expected trend, with complexes with electron withdrawing substituents, such as Br, being less thermodynamically likely to donate a hydride (higher thermodynamic hydricity) than complexes with an electron donating substituent, such as OMe. An exception to this is trend [(6,6'-(NHMe)<sub>2</sub>-bpy)Re(CO)<sub>3</sub>H], which is calculated to be less thermodynamically hydridic than unsubstituted [(bpy)Re(CO)<sub>3</sub>H] despite the presence of electron donating amine substituents. However, there is likely more error in the calculated

**Table 5:** Computed relative thermodynamic hydricities of [(R<sub>2</sub>-bpy)Re(CO)<sub>3</sub>H] determined through isodesmic exchange reactions with [(bpy)Re(CO)<sub>3</sub>(MeCN)]<sup>+</sup>.<sup>a</sup>

Relative Thermodynamic Hydricity (kcal mol-1)

Complex		Complex	
[(4,4'-(OMe) <sub>2</sub> -bpy)Re(CO) <sub>3</sub> H]	-0.9	[(6,6'-(OEt) <sub>2</sub> -bpy)Re(CO) <sub>3</sub> H]	-1.6
$[(4,4'\text{-}(^tBu)_2\text{-}bpy)Re(CO)_3H]$	-0.4	$[(6,6'\text{-}(OMe)_2\text{-}bpy)Re(CO)_3H]$	-1.0
$[(4,4'\text{-Me}_2\text{-bpy})Re(CO)_3H]$	-0.5	$[(6,6'\text{-}(NHMe)_2\text{-}bpy)Re(CO)_3H]$	0.4*
$[(4,4'\text{-H}_2\text{-bpy})\text{Re}(\text{CO})_3\text{H}]$	0.0	$[(6,6'\text{-Me}_2\text{-bpy})\text{Re}(\text{CO})_3\text{H}]$	0.0
$[(4,4'\text{-Br}_2\text{-bpy})\text{Re}(\text{CO})_3\text{H}]$	1.1	$[(6,6'-F_2-bpy)Re(CO)_3H]$	1.1
$[(4,4'\text{-}(COOMe)_2\text{-}bpy)Re(CO)_3H]$	0.9	$[(6,6'-Br_2-bpy)Re(CO)_3H]$	1.6
$[(4,4'\text{-}(CF_3)_2\text{-}bpy)Re(CO)_3H]$	1.7		

<sup>&</sup>lt;sup>a</sup>All computations were performed at the M06/def2-TZVP level with SMD continuum solvation model with MeCN as the solvent using optimized structures at the B3LYP-D3 level of theory in vacuum. \*For calculating the relative thermodynamic hydricity of  $[(6,6'-(NHMe)_2-bpy)Re(CO)_3H]$  we used the most thermodynamically stable conformers (in relation to the tilt of the  $6,6'-(NHMe)_2bpy$  ligand for  $[(6,6'-(NHMe)_2-bpy)Re(CO)_3H]$  and  $[(6,6'-(NHMe)_2-bpy)Re(CO)_3(MeCN)]^+$  (see SI for more details).

thermodynamic hydricity of  $[(6,6'-(NHMe)_2-bpy)Re(CO)_3H]$  because the up isomer is more stable for  $[(6,6'-(NHMe)_2-bpy)Re(CO)_3H]$ , while the down isomer is more stable for  $[(6,6'-(NHMe)_2-bpy)Re(CO)_3(MeCN)^+]$  (see section SXIII). Further, there is more variation in the relative thermodynamic hydricity of  $[(6,6'-(NHMe)_2-bpy)Re(CO)_3H]$  when the functional is changed (Table S4). There is no obvious trend in the computed relative thermodynamic hydricity values between complexes supported by 4,4'- and 6,6' substituted bpy ligands with the same substituents. For example, there is almost no change in relative thermodynamic hydricities for R = MeO substituent but there is a significant change for R = Recolor (Table 5). Although this can be partially explained by computational error it suggests that care needs to be taken in assuming the same quantitative trends between systems containing different 4,4'- and 6,6' substituted bpy ligands.

A Brønsted plot,<sup>27</sup> comparing the experimental rate constants for CO<sub>2</sub> insertion into [(6,6'-R<sub>2</sub>bpy)Re(CO)<sub>3</sub>H] (ln( $k_l$ )) with the thermodynamic driving force for the reaction (ln( $K_{eq}$ ), where  $K_{eq}$ is the equilibrium constant for CO<sub>2</sub> insertion derived from the calculated thermodynamic hydricity of [(6,6'-R<sub>2</sub>-bpy)Re(CO)<sub>3</sub>H] and the experimental hydride affinity of CO<sub>2</sub>), was generated (Figure 5 and see SI).<sup>28</sup> The plot shows that there is a reasonable LFER between kinetic and thermodynamic hydricity (see Figures S16 & S18 for plots with different functionals). Apart from [(6,6'-Me<sub>2</sub>-bpy)Re(CO)<sub>3</sub>H], which appears to be an outlier for unknown reasons (and is not included in the analysis), all of the other hydrides fit a linear trendline. The fact that [(6,6'-(NHMe)<sub>2</sub>-bpy)Re(CO)<sub>3</sub>H] fits relatively well to the trendline (especially given the challenges associated with calculating its thermodynamic hydricity), suggests that the N-H group in the ligand is not providing any stabilization of the TS through hydrogen bonding. Our results also indicate that for CO<sub>2</sub> insertion into our selection of Re hydrides, steric factors do not play a large role, as if they did, we would not expect a hydride with a 6,6'-F<sub>2</sub>-bpy ligand to fit on the same trendline as a hydride with a sterically larger 6,6'-OEt2-bpy ligand. A notable feature of the Brønsted plot is the relatively large slope (a value) of 0.85. This could lead to a conclusion that the reaction is proceeding through a stepwise rather than concerted mechanism, <sup>27d,29</sup> and is larger than the α value of 0.79, we previously reported for CO<sub>2</sub> insertion to [(4,4'-R<sub>2</sub>-bpy)Re(CO)<sub>3</sub>H].<sup>7</sup> However, we used a slightly different computational method in this work, as control studies suggest that it leads to better agreement in thermodynamic hydricity values, 9 and this impacts the α value. When a Brønsted plot was constructed with the new computational method for [(4,4'-R<sub>2</sub>bpy)Re(CO)<sub>3</sub>H] we observed an  $\alpha$  value of 1.08 (Figure 6). This suggests that the  $\alpha$  value is heavily

dependent on the computational method and care should be taken in its interpretation, as likely these reactions are proceeding through a concerted hydride transfer, as observed in many other studies and suggested by our own calculations (*vide supra*).<sup>26</sup>

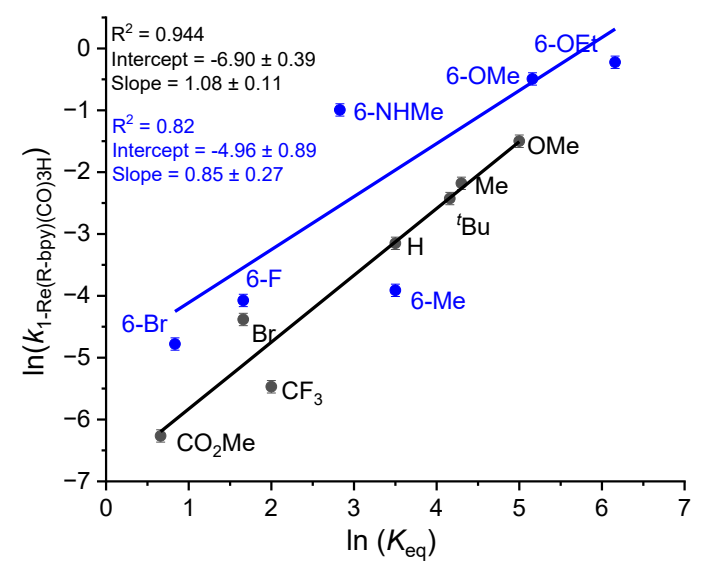


**Figure 6:** Brønsted plot showing the LFERs for CO<sub>2</sub> insertion into [(6,6'-R<sub>2</sub>-bpy)Re(CO)<sub>3</sub>H] (blue) and [(4,4'-R<sub>2</sub>-bpy)Re(CO)<sub>3</sub>H] (black). The fitting for [(6,6'-R<sub>2</sub>-bpy)Re(CO)<sub>3</sub>H] complexes is done excluding [(6,6'-Me<sub>2</sub>-bpy)Re(CO)<sub>3</sub>H].

When the LFER for CO<sub>2</sub> insertion into [(4,4'-R<sub>2</sub>-bpy)Re(CO)<sub>3</sub>H], which we previously reported, <sup>7</sup> is compared with the LFER for [(6,6'-R<sub>2</sub>-bpy)Re(CO)<sub>3</sub>H] two distinct trendlines are observed (Figure 6). Although the slopes are relatively similar, for a given thermodynamic hydricity, CO<sub>2</sub> insertion into a [(6,6'-R<sub>2</sub>-bpy)Re(CO)<sub>3</sub>H] complex is predicted to be faster than for a [(4,4'-R<sub>2</sub>-bpy)Re(CO)<sub>3</sub>H] complex. This is important because if the sole goal of this work was to break the scaling relationship between kinetic and thermodynamic hydricity for [(4,4'-R<sub>2</sub>-bpy)Re(CO)<sub>3</sub>H] complexes, the rate constant for CO<sub>2</sub> insertion for [(6,6'-(NHMe)<sub>2</sub>-bpy)Re(CO)<sub>3</sub>H], alongside its calculated thermodynamic hydricity, would have achieved that result. From this observation, a researcher could easily conclude that potential hydrogen bonding from the N–H group provides TS stabilization. However, upon expanding the scope of Re hydrides to include several control complexes with 6,6'-substituents on the bpy ligand that cannot participate in hydrogen bonding, a more accurate conclusion can be reached; that any substitution in the 6,6'-bpy position will likely break the scaling relationship for 4,4'-R<sub>2</sub>-bpy ligated systems. This is presumably a consequence of the tilting observed for 6,6'-R<sub>2</sub>-bpy systems, which fundamentally changes the bonding of the ligand to the metal and subsequently impacts the reactivity.

Using the experimental rates for hydride transfer from [(6,6'-R<sub>2</sub>-bpy)Re(CO)<sub>3</sub>H] to NMP<sup>+</sup> and the calculated thermodynamic hydricities for [(6,6'-R<sub>2</sub>-bpy)Re(CO)<sub>3</sub>H], we also constructed a Brønsted plot of hydride transfer from [(6,6'-R<sub>2</sub>-bpy)Re(CO)<sub>3</sub>H] to NMP<sup>+</sup> (see Figure S15). In this case, although the rate of hydride transfer generally increases with an increase in driving force, the correlation between thermodynamic and kinetic hydricity is relatively poor. This stands in contrast to our previous work where we showed that there is a strong LFER for hydride transfer from complexes of the type [(4,4'-R<sub>2</sub>-bpy)Re(CO)<sub>3</sub>H] to NMP<sup>+</sup>. Likely the poor correlation for [(6,6'-R<sub>2</sub>-bpy)Re(CO)<sub>3</sub>H] is due to steric factors, which are more pronounced for NMP<sup>+</sup> compared to CO<sub>2</sub>. Consistent with this proposal, [(6,6'-OEt<sub>2</sub>-bpy)Re(CO)<sub>3</sub>H] and [(6,6'-(NHMe)<sub>2</sub>bpy)Re(CO)<sub>3</sub>H], the most sterically bulky hydrides, are slower than would be expected based on the approximate trendline. In general, for a given thermodynamic hydricity, hydride transfer from [(4,4'-R<sub>2</sub>-bpy)Re(CO)<sub>3</sub>H] complexes to NMP<sup>+</sup> is faster than for [(6,6'-R<sub>2</sub>-bpy)Re(CO)<sub>3</sub>H] complexes. This is the opposite trend compared with CO<sub>2</sub>, which is again attributed to steric factors. Overall, our results highlight that in a similar fashion to [(4,4'-R2-bpy)Re(CO)<sub>3</sub>H] complexes, [(6,6'-R<sub>2</sub>-bpy)Re(CO)<sub>3</sub>H] complexes display LFERs for hydride transfer. However, different LFERs are observed for bpy ligands with 6,6'-substituents compared to systems with 4,4'bpy substituents and depending on the exact properties of the substrate, 6,6'-substituted bpy ligands can give either faster or slower hydride transfer. Based on the fact that 5,5'-substituents on bpy impact the electronic and steric properties differently from 4,4'- and 6,6'-substituents, it is likely that they will also give rise to unique LFERs.

#### **Conclusions**

In this work, we have synthesized a series of Re hydrides containing 6,6'-substituted bpy ancillary ligands. These complexes readily insert CO<sub>2</sub> to form Re formates. Analysis of the structures of the 6,6'-R<sub>2</sub>-bpy supported Re hydride and formate species using X-ray crystallography, MicroED, and computational methods reveals that the bpy ligands are tilted so that the aromatic rings are not coplanar with the metal coordination plane containing the two nitrogen donors of the bpy ligand. This tilting is likely due to steric factors and is not observed in related 4,4'-R<sub>2</sub>-bpy ligated complexes. The rate constants for CO<sub>2</sub> insertion into [(6,6'-R<sub>2</sub>-bpy)Re(CO)<sub>3</sub>H] and hydride transfer from [(6,6'-R<sub>2</sub>-bpy)Re(CO)<sub>3</sub>H] to NMP<sup>+</sup> were determined. Using calculated thermodynamic hydricities, we generated Brønsted plots showing a LFER between thermodynamic hydricity and kinetic hydricity. The correlation was significantly stronger for CO<sub>2</sub> compared to NMP<sup>+</sup> likely for

steric reasons. The most important conclusion from the LFERs is that the relationship for 6,6'-R<sub>2</sub>-bpy ligated complexes is different to those we previously determined for (4,4'-R<sub>2</sub>-bpy)Re(CO)<sub>3</sub>H complexes.<sup>7</sup> For example, at a given driving force, CO<sub>2</sub> insertion into 6,6'-R<sub>2</sub>-bpy ligated species is faster than for 4,4'-R<sub>2</sub>-bpy ligated systems. An immediate implication of this result is that substituents in the 6,6' positions of the bpy, such as NHMe, which could be proposed to result in an increase in rate due to hydrogen bonding, in fact cause an increase in rate because of a general effect related to 6,6'-substituents. Given the prevalence of bpy ligands in a wide-range of transformations ranging from organic processes, such as cross-electrophile coupling,<sup>30</sup> to reactions relevant to energy storage applications, such as water oxidation<sup>31</sup> and CO<sub>2</sub> reduction,<sup>32</sup> our fundamental studies on the impact of introducing 6,6'-substituents to bpy ligands are likely to be broadly applicable. They suggest that both the structure and reactivity of transition metal complexes are impacted in a non-intuitive fashion by the addition of 6,6'-substituents to bpy ligands.

# **Experimental and Computational Methods**

Unless otherwise stated, all reactions were carried out under a dinitrogen atmosphere using standard Schlenk procedures or a MBraun glovebox. NMR spectra were recorded on Agilent DD2 -400, -500, -600 spectrometers at ambient probe temperatures unless otherwise specified. IR spectra were collected on a FTIR/Raman Thermo Nicolet 6700 under air. UV-Vis characterization of authentic samples was performed on a Shimadzu UV-3600Plus under N<sub>2</sub>. All stopped-flow experiments were performed using a TgK Scientific Hi-Tech Scientific CryoStopped-Flow System (SF-61DX2) apparatus equipped with a diode array detector. The stopped-flow system was controlled by the Kinetic Studio 2.33 software. Observed rate constants from variable temperature stopped-flow experiments were derived using global analysis fitting with the SPECFIT/32 software. Calculations were performed in the Gaussian 16 software package. For further details about experimental and computational methods refer to the supporting information.

### Acknowledgments

NH acknowledges support from the National Science Foundation through Grants CHE-1953708 & CHE-2347883 and the Yale Center for Natural Carbon Capture. MRE acknowledges the support of the Natural Sciences and Engineering Research Council of Canada (NSERC), PDF-568014-2022. The work at Brookhaven National Laboratory (MZE) was carried out under contract DE-

SC0012704 with the U.S. Department of Energy, Office of Science, Office of Basic Energy Sciences, and utilized computational resources at the Center for Functional Nanomaterials, which is a U.S. Department of Energy Office of Science Facility, and the Scientific Data and Computing Center, a component of the Computational Science Initiative, at Brookhaven National Laboratory under Contract No. DE-SC0012704.

### **Supporting Information**

Additional experimental details, kinetic data, computational information, characterization details, NMR spectra.

# **Competing Financial Interests**

The authors declare no competing financial interests.

#### References

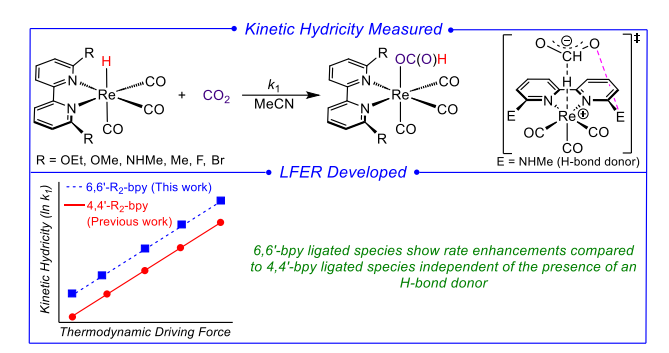
- 1. (a) Hoskin, A. J.; Stephan, D. W. Early Transition Metal Hydride Complexes: Synthesis and Reactivity. *Coord. Chem. Rev.* **2002**, *233*, 107; (b) McGrady, G. S.; Guilera, G. The Multifarious World of Transition Metal Hydrides. *Chem. Soc. Rev.* **2003**, *32*, 383; (c) Samec, J. S.; Bäckvall, J.-E.; Andersson, P. G.; Brandt, P. Mechanistic Aspects of Transition Metal-Catalyzed Hydrogen Transfer Reactions. *Chem. Soc. Rev.* **2006**, *35*, 237; (d) Norton, J. R.; Sowa, J. Introduction: Metal Hydrides. *Chem. Rev.* **2016**, *116*, 8315; (e) Humphries, T. D.; Sheppard, D. A.; Buckley, C. E. Recent Advances in the 18-Electron Complex Transition Metal Hydrides of Ni, Fe, Co and Ru. *Coord. Chem. Rev.* **2017**, *342*, 19; (f) Ai, W.; Zhong, R.; Liu, X.; Liu, Q. Hydride Transfer Reactions Catalyzed by Cobalt Complexes. *Chem. Rev.* **2018**, *119*, 2876.
- 2. (a) Bäckvall, J.-E. Transition Metal Hydrides as Active Intermediates in Hydrogen Transfer Reactions. *J. Organomet. Chem.* **2002**, *652*, 105; (b) Blaser, H. U.; Malan, C.; Pugin, B.; Spindler, F.; Steiner, H.; Studer, M. Selective Hydrogenation for Fine Chemicals: Recent Trends and New Developments. *Adv. Synth. Catal.* **2003**, *345*, 103; (c) Johnson, N. B.; Lennon, I. C.; Moran, P. H.; Ramsden, J. A. Industrial-Scale Synthesis and Applications of Asymmetric Hydrogenation Catalysts. *Acc. Chem. Res.* **2007**, *40*, 1291; (d) Wang, D.; Astruc, D. The Golden Age of Transfer Hydrogenation. *Chem. Rev.* **2015**, *115*, 6621; (e) Seo, C. S.; Morris, R. H. Catalytic Homogeneous Asymmetric Hydrogenation: Successes and Opportunities. *Organometallics* **2018**, *38*, 47; (f) Baidilov, D.; Hayrapetyan, D.; Khalimon, A. Y. Recent Advances in Homogeneous Base-Metal-Catalyzed Transfer Hydrogenation Reactions. *Tetrahedron* **2021**, *98*, 132435.
- 3. (a) Franke, R.; Selent, D.; Börner, A. Applied Hydroformylation. *Chem. Rev.* **2012**, *112*, 5675; (b) Wu, X.-F.; Fang, X.; Wu, L.; Jackstell, R.; Neumann, H.; Beller, M. Transition-Metal-Catalyzed Carbonylation Reactions of Olefins and Alkynes: A Personal Account. *Acc. Chem. Res.* **2014**, *47*, 1041; (c) Börner, A.; Franke, R. (Eds) *Hydroformylation: Fundamentals, Processes, and Applications in Organic Synthesis*, John Wiley & Sons, **2016**, Weinheim, Germany; (d) Nurttila, S. S.; Linnebank, P. R.; Krachko, T.; Reek, J. N. Supramolecular Approaches to Control Activity and Selectivity in Hydroformylation Catalysis. *ACS Catal.* **2018**, *8*, 3469; (e) Chakrabortty, S.; Almasalma, A. A.; de Vries, J. G. Recent Developments in Asymmetric Hydroformylation. *Catal. Sci. Technol.* **2021**, *11*, 5388; (f) Rodrigues, F. M.; Carrilho, R. M.; Pereira, M. M. Reusable Catalysts for Hydroformylation-Based Reactions. *Eur. J. Inorg. Chem.* **2021**, *2021*, 2294.
- 4. (a) Hilt, G. Double Bond Isomerisation and Migration—New Playgrounds for Transition Metal-Catalysis. *ChemCatChem* **2014**, *6*, 2484; (b) Larionov, E.; Li, H.; Mazet, C. Well-Defined Transition Metal Hydrides in Catalytic Isomerizations. *Chem. Commun.* **2014**, *50*, 9816; (c) Hassam, M.; Taher, A.; Arnott, G. E.; Green, I. R.; van Otterlo, W. A. Isomerization of Allylbenzenes. *Chem. Rev.* **2015**, *115*, 5462; (d) Vasseur, A.; Bruffaerts, J.; Marek, I. Remote Functionalization Through Alkene Isomerization. *Nature Chem.* **2016**, *8*, 209; (e) Massad, I.; Marek, I. Alkene Isomerization Through Allylmetals as a Strategic Tool in Stereoselective Synthesis. *ACS Catal.* **2020**, *10*, 5793; (f) Fiorito, D.; Scaringi, S.; Mazet, C. Transition Metal-Catalyzed Alkene Isomerization as an Enabling Technology in Tandem, Sequential and Domino Processes. *Chem. Soc. Rev.* **2021**, *50*, 1391.

- 5. (a) Nakajima, Y.; Shimada, S. Hydrosilylation Reaction of Olefins: Recent Advances and Perspectives. *RSC Adv.* **2015**, *5*, 20603; (b) Du, X.; Huang, Z. Advances in Base-Metal-Catalyzed Alkene Hydrosilylation. *ACS Catal.* **2017**, 7, 1227; (c) Obligacion, J. V.; Chirik, P. J. Earth-Abundant Transition Metal Catalysts for Alkene Hydrosilylation and Hydroboration. *Nature Rev. Chem.* **2018**, *2*, 15; (d) de Almeida, L. D.; Wang, H.; Junge, K.; Cui, X.; Beller, M. Recent Advances in Catalytic Hydrosilylations: Developments Beyond Traditional Platinum Catalysts. *Angew. Chem. Int. Ed.* **2021**, *60*, 550.
- 6. (a) Mochida, I.; Yoneda, Y. Linear Free Energy Relationships In Heterogeneous Catalysis: I. Dealkylation of Alkylbenzenes on Cracking Catalysts. *J. Catal.* **1967**, *7*, 386; (b) Bjelic, S.; Åqvist, J. Catalysis and Linear Free Energy Relationships in Aspartic Proteases. *Biochemistry* **2006**, *45*, 7709; (c) Miller, J. J.; Sigman, M. S. Quantitatively Correlating the Effect of Ligand-Substituent Size in Asymmetric Catalysis Using Linear Free Energy Relationships. *Angew. Chem. Int. Ed.* **2008**, *47*, 771; (d) Pothupitiya, J. U.; Hewawasam, R. S.; Kiesewetter, M. K. Urea and Thiourea H-bond Donating Catalysts for Ring-Opening Polymerization: Mechanistic Insights via (Non) Linear Free Energy Relationships. *Macromolecules* **2018**, *51*, 3203; (e) Lan, Z.; Sharada, S. M. A Framework for Constructing Linear Free Energy Relationships to Design Molecular Transition Metal Catalysts. *Phys. Chem. Chem. Phys.* **2021**, *23*, 15543. 7. Espinosa, M. R.; Ertem, M. Z.; Barakat, M.; Bruch, Q. J.; Deziel, A. P.; Elsby, M. R.; Hasanayn, F.; Hazari, N.; Miller, A. J.; Pecoraro, M. V. Correlating Thermodynamic and Kinetic Hydricities of Rhenium Hydrides. *J. Am. Chem. Soc.* **2022**, *144*, 17939.
- 8. (a) Hawecker, J.; Lehn, J.-M.; Ziessel, R. Electrocatalytic Reduction of Carbon Dioxide Mediated by Re(bipy)(CO)<sub>3</sub> Cl (bipy= 2,2'-bipyridine). J. Chem. Soc., Chem. Commun. 1984, 328; (b) Sullivan, B. P.; Bolinger, C. M.; Conrad, D.; Vining, W. J.; Meyer, T. J. One- and Two-Electron Pathways in the Electrocatalytic Reduction of CO2 by fac-Re(bpy)(CO)<sub>3</sub>Cl (bpy = 2,2'-bipyridine). J. Chem. Soc., Chem. Commun. 1985, 1414; (c) Kutal, C.; Corbin, A. J.; Ferraudi, G. Further Studies of the Photoinduced Reduction of Carbon Dioxide Mediated by Tricarbonylbromo(2,2'bipyridine)rhenium(I). Organometallics 1987, 6, 553; (d) Johnson, F. P. A.; George, M. W.; Hartl, F.; Turner, J. J. Electrocatalytic Reduction of CO<sub>2</sub> Using the Complexes [Re(bpy)(CO)<sub>3</sub>L]<sub>n</sub> (n = +1,  $L = P(OEt)_3$ ,  $CH_3CN$ ; n = 0,  $L = P(OEt)_3$ ,  $L = P(OET)_3$ , L = PCl<sup>-</sup>, OTf<sup>-</sup>; bpy = 2,2'-Bipyridine; OTf<sup>-</sup> = CF<sub>3</sub>SO<sub>3</sub>) as Catalyst Precursors: Infrared Spectroelectrochemical Investigation. Organometallics 1996, 15, 3374; (e) Smieja, J. M.; Kubiak, C. P. Re (bipy-tBu)(CO)-Cl- Improved Catalytic Activity for Reduction of Carbon Dioxide: IR-Spectroelectrochemical and Mechanistic Studies. *Inorg.* Chem. 2010, 49, 9283; (f) Keith, J. A.; Grice, K. A.; Kubiak, C. P.; Carter, E. A. Elucidation of the Selectivity of Proton-Dependent Electrocatalytic CO<sub>2</sub> Reduction by fac-Re(bpy)(CO)<sub>3</sub>Cl. J. Am. Chem. Soc. 2013, 135, 15823; (g) Sampson, M. D.; Froehlich, J. D.; Smieja, J. M.; Benson, E. E.; Sharp, I. D.; Kubiak, C. P. Direct Observation of the Reduction of Carbon Dioxide by Rhenium Bipyridine Catalysts. Energy Environ. Sci. 2013, 6, 3748; (h) Jia, X.; Nedzbala, H. S.; Bottum, S.; Cahoon, J. S.; Concepcion, J. J.; Donley, C.; Gang, A.; Han, Q.; Hazari, N.; Kessinger, M. C.; Lockett, M. R.; Mayer, J. M.; Mercado, B. Q.; Meyer, G. J.; Pearce, A. J.; Rooney, C. L.; Sampaio, R. N.; Shang, B.; Wang, H. Synthesis and Surface Attachment of Molecular Re(I) Complexes Supported by Functionalized Bipyridyl Ligands. Inorg. Chem. 2023, 62, 2359; (i) Jia, X.; Cui, K.; Alvarez-Hernandez, J. L.; Donley, C. L.; Gang, A.; Hammes-Schiffer, S.; Hazari, N.; Jeon, S.; Mayer, J. M.; Nedzbala, H. S.; Shang, B.; Stach, E. A.; Stewart-Jones, E.; Wang, H.; Williams, A. Synthesis and Surface Attachment of Molecular Re(I) Hydride Species with Silatrane Functionalized Bipyridyl Ligands. Organometallics 2023, 42, 2238.
- 9. Elsby, M. R.; Espinosa, M. R.; Ertem, M. Z.; Deziel, A. P.; Hazari, N.; Miller, A. J.; Paulus, A. H.; Pecoraro, M. V. Carbon Dioxide Insertion into Rhenium Hydrides as a Probe for the Impact of Solvent on Linear Free Energy Relationships between Thermodynamic and Kinetic Hydricity. *Organometallics* **2023**, *42*, 3005.
- 10. (a) Gerlt, J. A.; Kreevoy, M. M.; Cleland, W.; Frey, P. A. Understanding Enzymic Catalysis: The Importance of Short, Strong Hydrogen Bonds. *Chem. Biol.* **1997**, *4*, 259; (b) Bartlett, G. J.; Porter, C. T.; Borkakoti, N.; Thornton, J. M. Analysis of Catalytic Residues in Enzyme Active Sites. *J. Mol. Biol.* **2002**, *324*, 105; (c) Hanoian, P.; Liu, C. T.; Hammes-Schiffer, S.; Benkovic, S. Perspectives on Electrostatics and Conformational Motions in Enzyme Catalysis. *Acc. Chem. Res.* **2015**, *48*, 482; (d) Fried, S. D.; Boxer, S. G. Measuring Electric Fields and Noncovalent Interactions Using the Vibrational Stark Effect. *Acc. Chem. Res.* **2015**, *48*, 998; (e) Fried, S. D.; Bagchi, S.; Boxer, S. G. Extreme Electric Fields Power Catalysis in the Active Site of Ketosteroid Isomerase. *Science* **2014**, *346*, 1510; (f) Wu, Y.; Boxer, S. G. A Critical Test of the Electrostatic Contribution to Catalysis with Noncanonical Amino Acids in Ketosteroid Isomerase. *J. Am. Chem. Soc.* **2016**, *138*, 11890; (g) Lin, Y.-W. Rational Design of Metalloenzymes: From Single to Multiple Active Sites. *Coord. Chem. Rev.* **2017**, *336*, 1; (h) Fried, S. D.; Boxer, S. G. Electric Fields and Enzyme Catalysis. *Annu. Rev. Biochem* **2017**, *86*, 387.
- 11. (a) Helm, M. L.; Stewart, M. P.; Bullock, R. M.; DuBois, M. R.; DuBois, D. L. A Synthetic Nickel Electrocatalyst with a Turnover Frequency Above 100,000 s<sup>-1</sup> for H<sub>2</sub> Production. *Science* **2011**, *333*, 863; (b) Cook, S. A.; Borovik, A. Molecular Designs for Controlling the Local Environments Around Metal Ions. *Acc. Chem. Res.* **2015**, *48*, 2407; (c) Mahmudov, K. T.; Kopylovich, M. N.; da Silva, M. F. C. G.; Pombeiro, A. J. Non-Covalent Interactions in the

- Synthesis of Coordination Compounds: Recent Advances. Coord. Chem. Rev. 2017, 345, 54; (d) Creutz, S. E.; Peters, J. C. Exploring Secondary-Sphere Interactions in Fe-N<sub>x</sub>H<sub>y</sub> Complexes Relevant to N<sub>2</sub> Fixation. Chem. Sci. 2017, 8, 2321; (e) Hale, L. V.; Szymczak, N. K. Hydrogen Transfer Catalysis Beyond the Primary Coordination Sphere. ACS Catal. 2018, 8, 6446; (f) Reek, J. N.; de Bruin, B.; Pullen, S.; Mooibroek, T. J.; Kluwer, A. M.; Caumes, X. Transition Metal Catalysis Controlled by Hydrogen Bonding in the Second Coordination Sphere. Chem. Rev. 2022, 122, 12308. 12. (a) Chu, H. S.; Lau, C. P.; Wong, K. Y.; Wong, W. T. Intramolecular N-H---H-Ru Proton-Hydride Interaction in Ruthenium Complexes with (2-(Dimethylamino)ethyl)cyclopentadienyl (Dimethylamino)propyl)cyclopentadienyl Ligands. Hydrogenation of CO<sub>2</sub> to Formic Acid via the N-H---H-Ru Hydrogen-Bonded Complexes. Organometallics 1998, 17, 2768; (b) Matsubara, T.; Hirao, K. Density Functional Study on the Hydrido Migration to CO<sub>2</sub> and CS<sub>2</sub> of the (η<sup>5</sup>-C<sub>5</sub>H<sub>4</sub>(CH<sub>2</sub>)<sub>3</sub>NH<sub>3</sub><sup>+</sup>) MH(H<sub>2</sub>PCH<sub>2</sub>PH<sub>2</sub>)(M= Fe, Ru, and Os) Complexes Promoted by the Protonated Amine Arm. Which Path Does the Reaction Take, Abstraction or Insertion? Organometallics 2001, 20, 5759; (c) Schmeier, T. J.; Dobereiner, G. E.; Crabtree, R. H.; Hazari, N. Secondary Coordination Sphere Interactions Facilitate the Insertion Step in an Iridium (III) CO<sub>2</sub> Reduction Catalyst. J. Am. Chem. Soc. 2011, 133, 9274.
- 13. (a) Jeoung, J.-H.; Dobbek, H. Carbon Dioxide Activation at the Ni, Fe-Cluster of Anaerobic Carbon Monoxide Dehydrogenase. *Science* **2007**, *318*, 1461; (b) Haviv, E.; Azaiza-Dabbah, D.; Carmieli, R.; Avram, L.; Martin, J. M.; Neumann, R. A Thiourea Tether in the Second Coordination Sphere as a Binding Site for CO<sub>2</sub> and a Proton Donor Promotes the Electrochemical Reduction of CO<sub>2</sub> to CO Catalyzed by a Rhenium Bipyridine-Type Complex. *J. Am. Chem. Soc.* **2018**, *140*, 12451.
- 14. (a) Hellman, A. N.; Haiges, R.; Marinescu, S. C. Rhenium Bipyridine Catalysts with Hydrogen Bonding Pendant Amines for CO<sub>2</sub> Reduction. *Dalton Trans.* **2019**, *48*, 14251; (b) Karges, J.; Kalaj, M.; Gembicky, M.; Cohen, S. M. Re<sup>I</sup> Tricarbonyl Complexes as Coordinate Covalent Inhibitors for the SARS-CoV-2 Main Cysteine Protease. *Angew. Chem. Int. Ed.* **2021**, *60*, 10716.
- 15. Guilhem, J.; Pascard, C.; Lehn, J.-M.; Ziessel, R. Crystal and Molecular Structures of μ-hydrido-bis [fac-(2,2'-bipyridine)-tricarbonylrhenium (I)] chloride, fac-(2,2'-bipyridine) tricarbonyl-formatorhenium (I), and fac-(2,2'-bipyridine) tricarbonyl (cyanotri-hydroborato) rhenium (I). *J. Chem. Soc., Dalton Trans.* **1989**, 1449.
- 16. (a) Dubey, A.; Nencini, L.; Fayzullin, R. R.; Nervi, C.; Khusnutdinova, J. R. Bio-Inspired Mn(I) Complexes for the Hydrogenation of CO<sub>2</sub> to Formate and Formamide. *ACS Catal.* **2017**, *7*, 3864; (b) Madsen, M. R.; Jakobsen, J. B.; Rønne, M. H.; Liang, H.; Hammershøj, H. C. D.; Nørby, P.; Pedersen, S. U.; Skrydstrup, T.; Daasbjerg, K. Evaluation of the Electrocatalytic Reduction of Carbon Dioxide Using Rhenium and Ruthenium Bipyridine Catalysts Bearing Pendant Amines in the Secondary Coordination Sphere. *Organometallics* **2020**, *39*, 1480; (c) Ross, D. A.; Mapley, J. I.; Cording, A. P.; Vasdev, R. A.; McAdam, C. J.; Gordon, K. C.; Crowley, J. D. 6, 6'-Ditriphenylamine-2, 2'-Bipyridine: Coordination Chemistry and Electrochemical and Photophysical Properties. *Inorg. Chem.* **2021**, *60*, 11852; (d) Kjellberg, M.; Ohleier, A.; Thuéry, P.; Nicolas, E.; Anthore-Dalion, L.; Cantat, T. Photocatalytic Deoxygenation of N–O bonds with Rhenium Complexes: From the Reduction of Nitrous Oxide to Pyridine N-Oxides. *Chem. Sci.* **2021**, *12*, 10266; (e) Rotundo, L.; Ahmad, S.; Cappuccino, C.; Polyansky, D. E.; Ertem, M. Z.; Manbeck, G. F. A Dicationic fac-Re(bpy)(CO)<sub>3</sub>Cl for CO<sub>2</sub> Electroreduction at a Reduced Overpotential. *Inorg. Chem.* **2023**, *62*, 7877.
- 17. (a) Steiner, T. The Hydrogen Bond in the Solid State. *Angew. Chem. Int. Ed.* **2002**, *41*, 48; (b) Samuel, H.; Nweke-Mariazu, U.; Etim, E. Understanding Intermolecular and Intramolecular Hydrogen Bonds: Spectroscopic and Computational Approaches. *J. Chem. Rev.* **2023**, *5*, 439.
- 18. Wagner, G.; Pardi, A.; Wuethrich, K. Hydrogen Bond Length and Proton NMR Chemical Shifts in Proteins. *J. Am. Chem. Soc.* **1983**, *105*, 5948.
- 19. Crabtree, R. H. Recent Advances in Hydrogen Bonding Studies Involving Metal Hydrides. *J. Organomet. Chem.* **1998**, *557*, 111.
- 20. (a) Mu, X.; Gillman, C.; Nguyen, C.; Gonen, T. An Overview of Microcrystal Electron Diffraction (MicroED). *Annu. Rev. Biochem* **2021**, *90*, 431; (b) Saha, A.; Nia, S. S.; Rodríguez, J. A. Electron Diffraction of 3D Molecular Crystals. *Chem. Rev.* **2022**, *122*, 13883.
- 21. Jones, C. G.; Asay, M.; Kim, L. J.; Kleinsasser, J. F.; Saha, A.; Fulton, T. J.; Berkley, K. R.; Cascio, D.; Malyutin, A. G.; Conley, M. P. Characterization of Reactive Organometallic Species via MicroED. *ACS Cent. Sci.* **2019**, *5*, 1507. 22. MicroED data was also obtained for [(6,6'-Br<sub>2</sub>-bpy)Re(CO)<sub>3</sub>H], [(6,6'-(OEt)<sub>2</sub>-bpy)Re(CO)<sub>3</sub>H], and [(6,6'-(OMe)<sub>2</sub>-bpy)Re(CO)<sub>3</sub>H] but was not of sufficient quality to yield structural information for publication. Nevertheless, the fact that diffraction data could be obtained on samples that could not be analyzed using X-ray diffraction highlights the advantages of MicroED.

- 23. Zhao, Y.; Truhlar, D. G. The M06 Suite of Density Functionals for Main Group Thermochemistry, Thermochemical Kinetics, Noncovalent Interactions, Excited States, and Transition Elements: Two New Functionals and Systematic Testing of Four M06-Class Functionals and 12 Other Functionals. *Theor. Chem. Acc.* **2008**, *120*, 215.
- 24. Sullivan, B. P.; Meyer, T. J. Kinetics and Mechanism of Carbon Dioxide Insertion into a Metal-Hydride Bond. A Large Solvent Effect and an Inverse Kinetic Isotope Effect. *Organometallics* **1986**, *5*, 1500.
- 25. Clark, M. L.; Cheung, P. L.; Lessio, M.; Carter, E. A.; Kubiak, C. P. Kinetic and Mechanistic Effects of Bipyridine (bpy) Substituent, Labile Ligand, and Brønsted Acid on Electrocatalytic CO<sub>2</sub> Reduction by Re (bpy) Complexes. *ACS Catal.* **2018**, *8*, 2021.
- 26. (a) Hazari, N.; Heimann, J. E. Carbon Dioxide Insertion into Group 9 and 10 Metal–Element σ Bonds. *Inorg. Chem.* 2017, 56, 13655; (b) Heimann, J. E.; Bernskoetter, W. H.; Hazari, N.; Mayer, James M. Acceleration of CO<sub>2</sub> Insertion into Metal Hydrides: Ligand, Lewis Acid, and Solvent Effects on Reaction Kinetics. *Chem. Sci.* 2018, 9, 6629; (c) Heimann, J. E.; Bernskoetter, W. H.; Hazari, N. Understanding the Individual and Combined Effects of Solvent and Lewis Acid on CO<sub>2</sub> Insertion into a Metal Hydride. *J. Am. Chem. Soc.* 2019, 141, 10520.
- 27. (a) Kreevoy, M. M.; Lee, I. S. H. Marcus Theory of a Perpendicular Effect on α for Hydride Transfer Between NAD<sup>+</sup> Analogs. *J. Am. Chem. Soc.* **1984**, *106*, 2550; (b) Ostovic, D.; Lee, I. S. H.; Roberts, R. M. G.; Kreevoy, M. M. Hydride Transfer and Oxyanion Addition Equilibria of NAD<sup>+</sup> Analogs. *J. Org. Chem.* **1985**, *50*, 4206; (c) Kreevoy, M. M.; Ostovic, D.; Lee, I. S. H.; Binder, D. A.; King, G. W. Structure Sensitivity of the Marcus λ Parameter for Hydride Transfer Between NAD<sup>+</sup> Analogs. *J. Am. Chem. Soc.* **1988**, *110*, 524; (d) Kim, Y.; Truhlar, D. G.; Kreevoy, M. M. An Experimentally Based Family of Potential Energy Surfaces for Hydride Transfer Between NAD<sup>+</sup> Analogs. *J. Am. Chem. Soc.* **1991**, *113*, 7837; (e) Lee, I.-S. H.; Jeoung, E. H.; Kreevoy, M. M. Marcus Theory of a Parallel Effect on α for Hydride Transfer Reaction between NAD<sup>+</sup> Analogues. *J. Am. Chem. Soc.* **1997**, *119*, 2722; (f) Han Lee, I.-S.; Jeoung, E. H.; Kreevoy, M. M. Primary Kinetic Isotope Effects on Hydride Transfer from 1,3-Dimethyl-2-phenylbenzimidazoline to NAD<sup>+</sup> Analogues. *J. Am. Chem. Soc.* **2001**, *123*, 7492.
- 28. The hydride transfer reaction to CO<sub>2</sub> results in a product in which the formate anion is coordinated to Re. In previous work, see reference 7, we have considered formate binding to the metal center when determining the overall thermodynamic favorability of CO<sub>2</sub> insertion. This is often referred to as the effective thermodynamic hydricity. In this work, we are most interested in the linear nature of the Brønsted plot, which is not affected by formate binding. Thus, we have not considered effective thermodynamic hydricity, which can only be easily determined in this case using computational methods. Instead, we have used the driving force estimated based on formate having a thermodynamic hydricity of 44 kcal mol<sup>-1</sup> (see: Brereton, K. R.; Smith, N. E.; Hazari, N.; Miller, A. J. M. Thermodynamic and Kinetic Hydricity of Transition Metal Hydrides. *Chem. Soc. Rev.* **2020**, *49*, 7929). For the sake of comparison, we have performed the same analysis for [(4,4'-R<sub>2</sub>-bpy)Re(CO)<sub>3</sub>H] complexes using the rate constants for CO<sub>2</sub> insertion previously determined in reference 7. See SI for more details.
- 29. Lee, I.-S. H.; Chow, K.-H.; Kreevoy, M. M. The Tightness Contribution to the Brønsted α for Hydride Transfer between NAD<sup>+</sup> Analogues. *J. Am. Chem. Soc.* **2002**, *124*, 7755.
- 30. (a) Everson, D. A.; Weix, D. J. Cross-Electrophile Coupling: Principles of Reactivity and Selectivity. *J. Org. Chem.* **2014**, *79*, 4793; (b) Weix, D. J. Methods and Mechanisms for Cross-Electrophile Coupling of Csp<sup>2</sup> Halides with Alkyl Electrophiles. *Acc. Chem. Res.* **2015**, *48*, 1767.
- 31. Blakemore, J. D.; Crabtree, R. H.; Brudvig, G. W. Molecular Catalysts for Water Oxidation. *Chem. Rev.* **2015**, *115*, 12974.
- 32. (a) Collin, J. P.; Sauvage, J. P. Electrochemical Reduction of Carbon Dioxide Mediated by Molecular Catalysts. *Coord. Chem. Rev.* **1989**, *93*, 245; (b) Francke, R.; Schille, B.; Roemelt, M. Homogeneously Catalyzed Electroreduction of Carbon Dioxide—Methods, Mechanisms, and Catalysts. *Chem. Rev.* **2018**, *118*, 4631; (c) Nandal, N.; Jain, S. L. A Review on Progress and Perspective of Molecular Catalysis in Photoelectrochemical Reduction of CO<sub>2</sub>. *Coord. Chem. Rev.* **2022**, *451*, 214271.

# **TOC Graphic**



# **Synopsis**

[ $(6,6'-R_2-bpy)Re(CO)_3H$ ] (bpy = 2,2'-bipyridine) complexes with different substituents were prepared and the rate constants for  $CO_2$  insertion to form the formate complexes [ $(6,6'-R_2-bpy)Re(CO)_3\{OC(O)H\}$ ] determined. A Brønsted plot was constructed using the rate constants for  $CO_2$  insertion and the thermodynamic hydricities for [ $(6,6'-R_2-bpy)Re(CO)_3H$ ]. There is a linear free energy relationship between thermodynamic and kinetic hydricity but it is different to that previously determined for [ $(4,4'-R_2-bpy)Re(CO)_3H$ ] and independent of potential hydrogen bonding in the secondary coordination sphere.